IOP Publishing Measurement Science and Technology
Meas. Sci. Technol. **31** (2020) 045002 (12pp) https://doi.org/10.1088/1361-6501/ab502e

Iterative alignment of reflector panels for large-scale compact test range in non-metrology environment based on laser tracker

Mingming Wang, Dongsheng Li and Youlei Zhao

School of Mechanical Engineering and Automation, Beihang University, Beijing, People's Republic of China

E-mail: wmm704@buaa.edu.cn

Received 20 July 2019, revised 17 October 2019
Accepted for publication 22 October 2019
Published 6 January 2020

Abstract

The reflector panel used for a large-scale compact test range (CTR) is usually divided into several sub-panels with appropriate size to be fabricated separately, and then these sub-panels are assembled and aligned for a long period to form a high-precision reflective surface. Toward that end, an iterative alignment system is established to accomplish alignment of reflector panels based on commercial laser tracker and 6-degree-of-freedom adjustment mechanism. The alignment is a very challenging task involving two aspects: coordinate system alignment and measurement uncertainty evaluation, especially in a non-metrology environment. For the former, an alignment method is developed to unify the measurement coordinate system of the system based on iteratively adding and modifying reference points. For the latter, the actual uncertainty model of laser tracker based on a large amount of field measurement data is analyzed and established using statistical analysis. Based on the uncertainty model, the measurement and alignment error is evaluated and verified by Monte Carlo simulations. As verification, 15 sub-panels of the CTR reflector with 12 m width and 7 m height are opportunely assembled and aligned using the iterative alignment system and algorithm. The final root-mean-square error of the deviation between the actual and theoretical profiles is achieved at 0.041 mm, where the accuracy loss caused by alignment is only 7.9% of the theoretical value. Results show that the alignment system and method proposed in this paper is effective and efficient to align the reflector panels for large-scale CTR in a non-metrology environment.

Keywords: iterative alignment, measurement uncertainty, reflector panels, laser tracker, non-metrology environment

(Some figures may appear in colour only in the online journal)

1. Introduction

High-accuracy reflector panels are important devices applied in a compact-test-range (CTR) system, the surface accuracy and dimension directly determine the quality of plane waves and the size of the quiet zone [1, 2]. Owing to limitations in equipment capacity, transportation capacity, and accuracy requirements, a large-scale reflector for the CTR is usually divided into several sub-panels with suitable size to be fabricated, and then these sub-panels are individually assembled and aligned to form a high-accuracy reflecting surface using advanced measuring equipment and appropriate measurement methods [3–5]. Measurement errors caused by the alignment process are unavoidable, especially in non-ideal measurement environments. For the large-scale reflector, on-site assembly and alignment is a long-lasting and challenging job. Therefore,

it is meaningful to study the appropriate method to reduce the alignment error in building the CTR.

The alignment accuracy of the reflector panels has a strong relationship with the accuracy of the measuring equipment and choice of measuring methods. On-site alignment of reflector panels calls for high-accuracy measurement devices and quantitative methods. With the development of measurement technology, the theodolite-tape method, a radio holographic or microwave holograph method, photographic measurement and laser tracker measurement are sequentially used to align the reflector panels [6–8]. Earlier, the theodolite-tape method was widely used in the measurement of the reflector of millimeter-wave antennas. Antennas using this method include the ARAM Φ30 m antenna, the assembly accuracy of which is ±0.12 mm [9], and seven Φ22 m telescopes in Australian, the surface accuracy of which is ±0.25 mm [10]. The largest-diameter antenna measured by this method is the Effelsberg antenna in Germany, and its measurement accuracy is better than ±1 mm within Φ80 m [11]. The theodolite-tape method is more suitable for the initial coarse alignment stage of an antenna. As an accuracy adjustment method and deformation monitoring method for improving the surface accuracy of an antenna reflector, the radio holographic or microwave holograph method has been applied more and more [12, 13]. The surface accuracy of the Φ100 m Effelsberg antenna was increased to ±0.50 mm by radio holographic or microwave holograph method [11]. Similarly, the surface accuracy of the IRAM Φ30 m antenna is increased from ±0.12 to ±0.08 mm [9]. Radio holography cannot be used for initial installation of antennas, and is more suitable for measurement alignment of large antennas. Small-caliber antennas are less accurate than optical measurement systems.

The laser tracker is a kind of measurement devices, featuring in high-speed, dynamic and high-accuracy characteristics, and is widely used in geometric measurements, such as antenna alignment, automotive fabrication and aircraft assembly [14]. The alignment of large-scale reflector panels referred to in [4, 5, 7] are all carried out using a commercial laser tracker in an undisturbed environment. However, these investigations do not offer any strategy to align the reflector panels in non-metrology environment. The laser tracker is an independent coordinate measuring system, and unifying measurement coordinate system is the key to the alignment of the reflector panels. The coordinate system alignment is usually achieved through common points placed on a stable foundation [15–17]. The global alignment of the LMT primary surface was attempted using a laser tracker in a non-metrology environment by setting fiducial points [18, 19]. However, such methods are not able to solve the problem of alignment in a periodic oscillation environment as it is very difficult to find a stable foundation for establishing reference points.

Through comprehensive analysis of previous research and problems encountered in this project, an iterative alignment system based on a commercial laser tracker and 6 degree-of-freedom (DOF) adjustment mechanism was proposed to solve the problem of on-site alignment of reflector panels in a non-metrology environment. In section 2, the alignment system composition is first introduced, and then the method of a unifying measurement coordinate system (MCS) is proposed. The methods for establishing a measurement uncertainty model of the laser tracker and evaluating the alignment error method of the unifying MCS are also presented in this section. In section 3, the application of the iterative alignment system for the alignment of reflector panels in a non-metrology environment is described. The process and results of on-site alignment of reflector panels for the CTR are presented, and then a microwave amplitude and phase test system based on probe scanning is established to evaluate electromagnetic performance of the CTR. Some conclusions are provided in section 4.

2. Iterative alignment system

2.1. System composition

It is a great challenge to accomplish the alignment of reflector panels for a large-scale CTR, especially in a non-metrology environment [5]. An iterative alignment system based on a commercial laser tracker and 6-DOF adjustment mechanism is established to accomplish the alignment of the reflector panels of the CTR. The actual profile data of each sub-panel are measured by the laser tracker, and then the positional deviation between the actual and theoretical profiles are calculated. According to this deviation value, the spatial posture of each sub-panel is adjusted by the 6-DOF adjustment mechanism. The alignment system is shown schematically in figure 1.

Each sub-panel is connected to a supporting structure by four adjustment mechanisms. The mechanism has the ability of precisely adjusting and locating in 6 DOFs. The position and posture of each panel is easily adjusted by a spatial parallel mechanism constituted by four mechanisms. To assist on-site installation and alignment of reflector panels, four Φ1.2 mm small holes called mark points are drilled on the face sheet, and are used in installing the mount base for a 0.5-in TBR. The deviation value of the offset on the mount base should be less than 2 μm when the 0.5-in TBR is placed at any angle. There are four Φ2.0 mm holes at the projection position on the back sheet that are used to roughly locate the adjustment mechanism. The mount base is pasted in the mark hole by hot melts, and is used to place the 0.5-in TBR in the process of measurement and alignment.

The challenge of this alignment system lies mainly in two issues: measurement accuracy of the laser tracker and adjustment accuracy of the 6-DOF mechanism. The positioning accuracy of the mechanism can reach 2 μm through operation by skilled workers. The adjustment value of each mechanism is calculated according to the measurement data of the laser tracker, and the adjustment process is monitored by the laser tracker in real time. Therefore, evaluating measurement uncertainty and unifying the MCS of the laser tracker is extremely important for the alignment of reflector panels in the long-period alignment process.

2.2. Iterative alignment algorithm

The first task of alignment for the reflector panels is to establish the accurate conversion relationship between the MCS

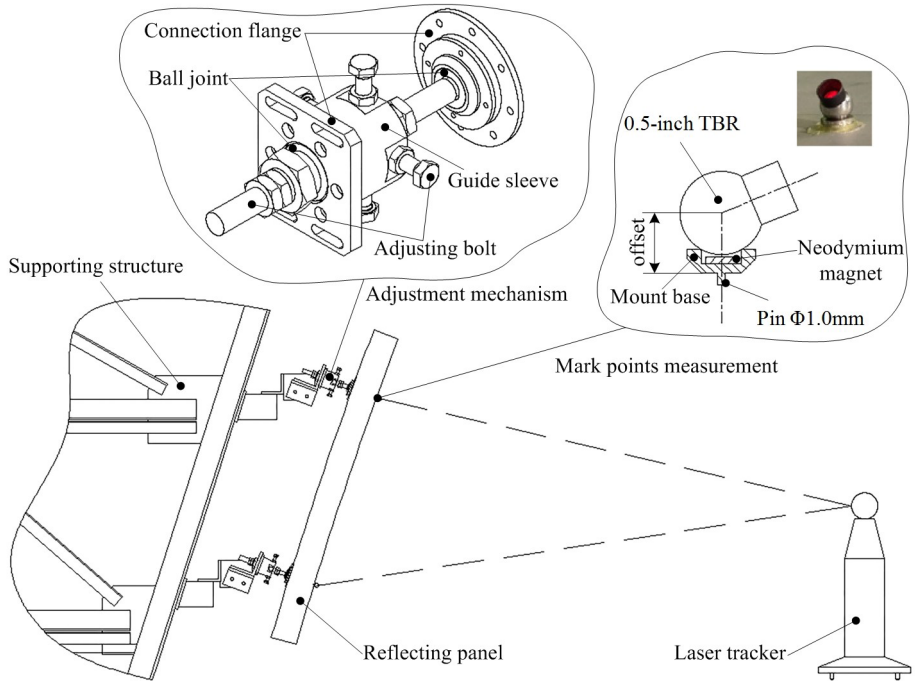

Figure 1. Iterative alignment system based on commercial laser tracker and 6-DOF adjustment mechanism.

and design coordinate system (DCS) when realizing the alignment of the reflector panels using the laser tracker. The relationship can be expressed as

$$\begin{bmatrix} X_{\mathrm{D}} \\ Y_{\mathrm{D}} \\ Z_{\mathrm{D}} \end{bmatrix} = \boldsymbol{R} * \begin{bmatrix} X_{\mathrm{M}} \\ Y_{\mathrm{M}} \\ Z_{\mathrm{M}} \end{bmatrix} + \boldsymbol{T} \tag{1}$$

where $O - X_{\mathrm{D}}Y_{\mathrm{D}}Z_{\mathrm{D}}$ is the DCS of the reflector, $O - X_{\mathrm{M}}Y_{\mathrm{M}}Z_{\mathrm{M}}$ the MCS of the laser tracker, $\boldsymbol{R}$ a rotation matrix, and $\boldsymbol{T}$ a translation matrix. Once the relationship is established, $\boldsymbol{R}$ and $\boldsymbol{T}$ will not change if the measuring environment is ideal. However, the ideal situation generally does not exist in the actual work scenario, resulting in simultaneous transformation of the rotation matrix R and the translation matrix T. The adjusted relationship is formulated as follows:

$$\begin{bmatrix} X_{\mathrm{D}} \\ Y_{\mathrm{D}} \\ Z_{\mathrm{D}} \end{bmatrix} = \boldsymbol{R}_0 \left(\boldsymbol{R} * \begin{bmatrix} X_{\mathrm{M}} \\ Y_{\mathrm{M}} \\ Z_{\mathrm{M}} \end{bmatrix} + \boldsymbol{T} \right) + \boldsymbol{T}_{\boldsymbol{0}} \tag{2}$$

where the rotation matrix $\boldsymbol{R}_0$ and translation matrix $\boldsymbol{T}_0$ represent the drift of the coordinate system caused by a non-metrology environment. How to avoid the influence of a non-metrology environment is the key issue in the alignment process of the reflector panels. Generally, the coordinate system is unified by reference points placed on high-stability foundations. However, it is difficult in this type of project to find a high-stability foundation on which to set the points in the non-metrology environment. Considering such a condition, in this paper we attempt to use a alignment method to unify the MCS using mark points on each reflection panel which were originally designed to facilitate inspection of the adjustment value of on-site alignment. The alignment process is briefly illustrated as follows. The first reflector panel is aligned to its unique nominal surface in the initial coordinate system. If the alignment accuracy meets the requirements, the mark points on the panel are measured immediately and put into a collection called reference points that is used to modify the MCS at the beginning of the alignment for the next panel. The detailed process of on-site alignment for reflector panels based on this self-modifying method is shown in figure 2. In the flowchart, $\mathbf{X}_{p,i}^{T_1}$ are the measurement values of the reference points at the end of the T_1 alignment period, and $\mathbf{X}_{p,i}^{T_2}$ the

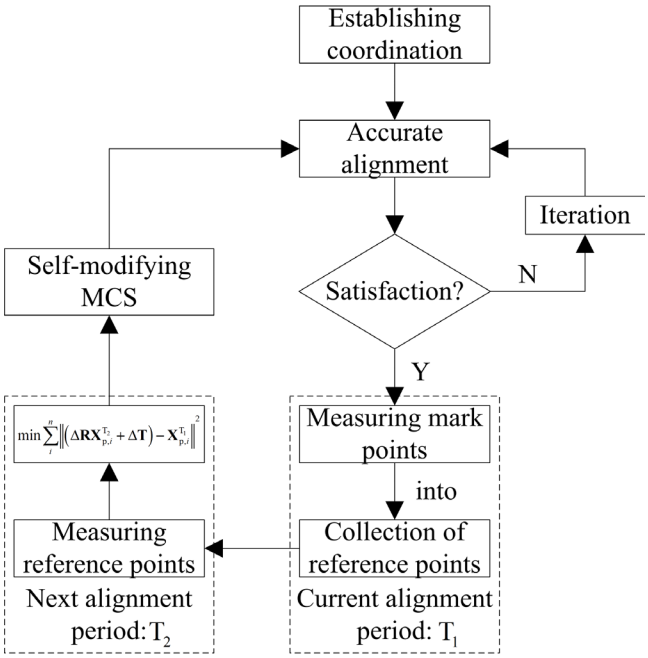

Figure 2. Alignment flow of reflector panels in non-metrology environment.

measurement values of the identical points at the beginning of the T_2 alignment period.

MCS drift caused by the non-metrology environment could be corrected and regressed through regression and a unified process shown in figure 2. However, due to measurement uncertainty of the laser tracker, each MCS alignment will introduce an alignment error. Therefore, the error introduced by each MCS regression must be quantitatively evaluated.

Let y_i indicate the coordinate value of the reference points under the T_1 alignment period and Δy_i the measurement error of the laser tracker. Similarly, x_i is the coordinate value of the reference points under the T_2 alignment period and Δx_i the measurement error. Thus, the MCS regression error (RE) is expressed as

$$\begin{aligned}\mathrm{RE} &= \sqrt{\frac{1}{n}\sum_{i=1}^{n}\left|\boldsymbol{R}'\left(x_i+\Delta x_i\right)+\boldsymbol{T}'-\left(y_i+\Delta y_i\right)\right|^2}\\ &= \sqrt{\frac{1}{n}\sum_{i=1}^{n}\left|\left(\boldsymbol{R}'x_i+\boldsymbol{T}'-y_i\right)+\Delta\varepsilon_i\right|^2}.\end{aligned} \tag{3}$$

Assuming there is no measurement error, a perfect match can be achieved between y_i and x_i:

$$y_i = \boldsymbol{R}_0 x_i + \boldsymbol{T}_0. \tag{4}$$

Substituting equation (4) into equation (3), the RE is rewritten as

$$\begin{aligned}\mathrm{RE} &= \sqrt{\frac{1}{n}\sum_{i=1}^{n}\left|\boldsymbol{R}'\left(x_i+\Delta x_i\right)+\boldsymbol{T}'-\left(\boldsymbol{R}_0x_i+\boldsymbol{T}_0+\Delta y_i\right)\right|^2}\\ &= \sqrt{\frac{1}{n}\sum_{i=1}^{n}\left|\left(R'x_i-\boldsymbol{R}_0x_i+\boldsymbol{T}'-\boldsymbol{T}_0\right)+\left(\boldsymbol{R}'\Delta x_i-\Delta y_i\right)\right|^2}\\ &= \sqrt{\frac{1}{n}\sum_{i=1}^{n}\left|\overline{\Delta\boldsymbol{R}}X_i+\Delta\boldsymbol{T}+\Delta\varepsilon_i\right|^2}.\end{aligned} \tag{5}$$

Assume that $\Delta\varphi, \Delta\theta, \Delta\kappa$ are rotation angles around the X, Y, and Z axes, respectively, and $\Delta t_x, \Delta t_y, \Delta t_z$ translation amounts along the X, Y, and Z axes, respectively. Since the measurement accuracy of the laser tracker is very high, the rotation-angle deviation is a high-order infinitesimal amount relative to the coordinate value. The rotation-parameter error matrix can be expressed as a Taylor approximation:

$$\overline{\Delta R} = \Delta R - I = \begin{bmatrix}0 & -\Delta\kappa & \Delta\theta\\ \Delta\kappa & 0 & -\Delta\varphi\\ -\Delta\theta & \Delta\varphi & 0\end{bmatrix} - I \tag{6}$$

$$\Delta T = T - T_0 = \left[\Delta t_x, \Delta t_y, \Delta t_z\right]^T \tag{7}$$

$$X_i = R_0 x_i \tag{8}$$

$$\Delta\varepsilon_i = R'\Delta x_i - \Delta y_i. \tag{9}$$

The minimization problem of equation (5) is actually consistent with solving the least-squares solution of the following equation sets.

$$\left.\begin{aligned}\overline{\Delta R}X_0+\Delta T &= -\Delta\varepsilon_0\\ \overline{\Delta R}X_1+\Delta T &= -\Delta\varepsilon_1\\ &\vdots\\ \overline{\Delta R}X_n+\Delta T &= -\Delta\varepsilon_n\end{aligned}\right\}. \tag{10}$$

Define configuration matrix C of reference points,

$$C = \begin{bmatrix}Z_1 & I_3\\ \vdots & \vdots\\ Z_i & I_3\\ \vdots & \vdots\\ Z_n & I_3\end{bmatrix} \tag{11}$$

where

$$Z_i = \begin{bmatrix}0 & X_{iz} & X_{iy}\\ -X_{iz} & 0 & X_{ix}\\ X_{iy} & -X_{ix} & 0\end{bmatrix}. \tag{12}$$

Equation (10) can be represented by a matrix form:

$$Cq = e \tag{13}$$

where q is the error matrix of the MCS alignment.

$$q = \left[\Delta\varphi, \Delta\theta, \Delta\kappa, \Delta t_x, \Delta t_y, \Delta t_z\right]^T \tag{14}$$

where e is the measurement error matrix of reference points:

$$e = \left[\Delta\varepsilon_{1x}, \Delta\varepsilon_{1y}, \Delta\varepsilon_{1z}, \cdots, \Delta\varepsilon_{ix}, \Delta\varepsilon_{iy}, \Delta\varepsilon_{iz}\right]^T. \tag{15}$$

Performing singular value decomposition of matrix C:

$$C = U\Lambda V. \tag{16}$$

Thus, the effective solution of the equation (10) is

$$q_{\min} = C^+ e \tag{17}$$

in which

$$C^+ = V\Lambda^+ U^T. \tag{18}$$

Therefore, the minimum value of the RE can be expressed in the following matrix form:

$$\mathrm{RE}_{\min} = e - Cq_{\min} = U\begin{bmatrix}0 & 0\\ 0 & I_{3n-6}\end{bmatrix}U^T e. \tag{19}$$

2.3. Measurement error model of laser tracker

The laser tracker is a typical spherical coordinate measuring system, and the coordinate value $\boldsymbol{x}$ in the Cartesian coordinate system can be expressed as a composite function of the sensor variable $\xi = \left[\alpha, \quad \beta, \quad d\right]^T$:

$$x = f\left(\xi\right) = \begin{bmatrix}d & \sin\beta & \cos\alpha\\ d & \sin\beta & \sin\alpha\\ d & \cos & \beta\end{bmatrix}. \tag{20}$$

The measurement uncertainty of the laser tracker is a random error mainly caused by distance measurement error of the laser and angle measurement error of the angle sensor. The coordinate measurement error Δx of the laser tracker can be expressed as

$$\Delta x = J\left(\xi\right)\Delta\xi \tag{21}$$

where $J\left(\xi\right)$ is the Jacques matrix and $\Delta\xi$ the distance error and angle error matrix:

$$J\left(\xi\right) = \begin{bmatrix}-d\sin\alpha\sin\beta & d\cos\alpha\cos\beta & \cos\alpha\cos\beta\\ d\cos\alpha\sin\beta & d\sin\alpha\cos\beta & \sin\alpha\sin\beta\\ 0 & -d\sin\beta & \cos\beta\end{bmatrix} \tag{22}$$

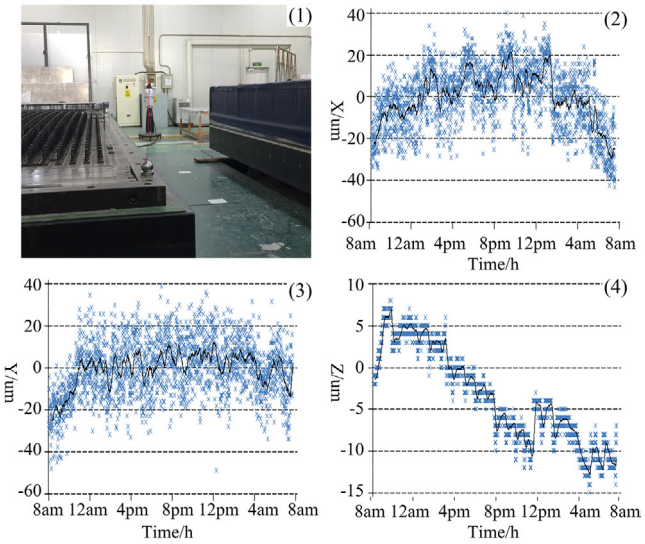

Figure 3. Actual measurement uncertainty of the laser tracker at laboratory environment with constant temperature (21 °C ± 1 °C) and constant humidity (50% ± 10%) and isolated foundation.

$$\Delta\xi = \left[\Delta\alpha, \quad \Delta\beta, \quad \Delta d\right]^T. \tag{23}$$

To establish the measurement error model of the laser tracker, several dynamic monitoring and measuring experiments were carried out. First, we operated the laser tracker (Lecia, AT901-B) to dynamically monitor and measure one reference point lasting 24 h in a laboratory environment with constant temperature (21 °C ± 1 °C) and constant humidity (50% ± 10%) and isolated vibration. The point was measured every 30 s, and the measurement distance is approximately 10 m. After 24 h monitoring and measurement, more than 2800 sets of data collected were statistically analyzed to evaluate the measurement uncertainty of the laser tracker. The measurement process and X, Y, Z coordinate fluctuations are shown in figure 3. According to the measurement characteristics of the laser tracker, measurement errors $\Delta\alpha, \Delta\beta, \Delta d$ of the angle and distance are irrelevant and random. Therefore, the normal analysis method was adopted to statistically analyze the measured parameters to establish the error model of the laser tracker. As is known from normal analysis, the measurement error $\Delta\alpha$ of the horizontal angle obeys a normal distribution with a standard deviation of $0.2558''$ and an average value of 0, while the measurement error $\Delta\beta$ of the vertical angle obeys a normal distribution with a standard deviation of $0.2855''$ and an average value of 0. The measurement error Δd of the laser distance obeys a normal distribution with standard deviations of 2.196 and 2.643 mm. The normal distribution curve of measurement errors $\Delta\alpha, \Delta\beta, \Delta d$ is shown in figure 4.

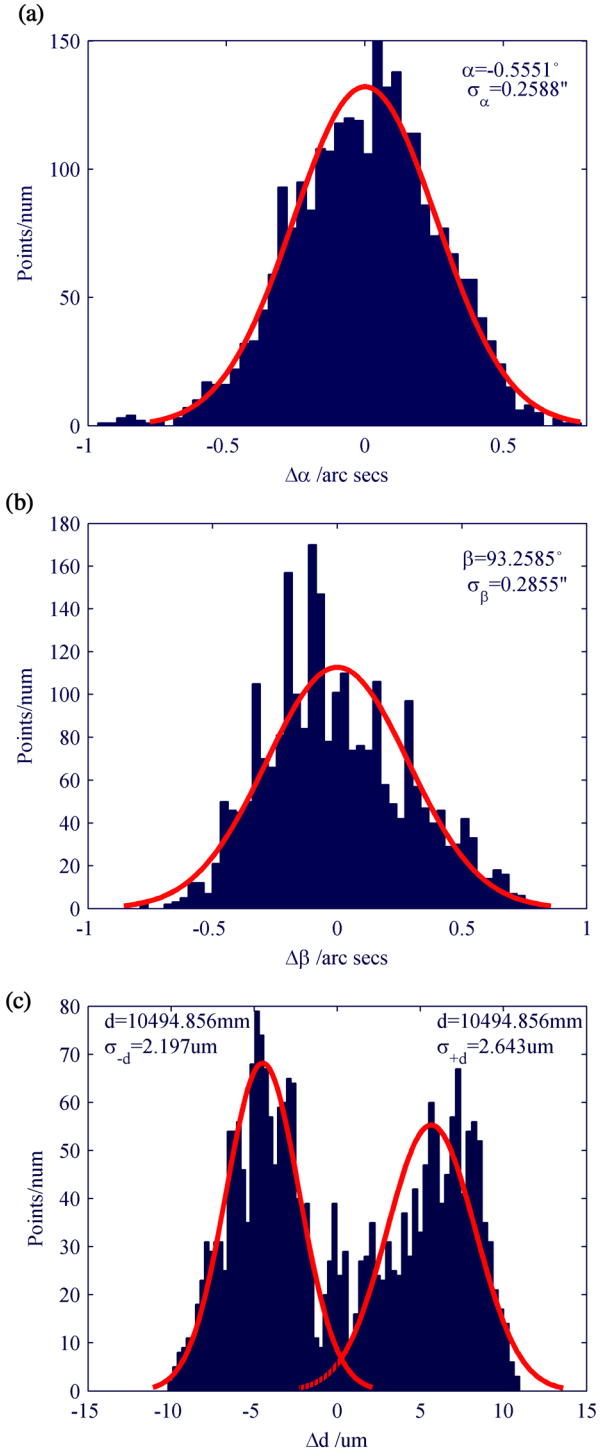

Figure 4. Error distribution of actually measuring a space point using lecia AT901-B. (a) Normal distribution fitting of horizontal angle error $\Delta\alpha$. (b) Normal distribution fitting of vertical angular error $\Delta\beta$. (c) Normal distribution fitting of interferometer distance error Δd.

3. Application and results

3.1. Electrical and structural design of reflector

A large-scale CTR was designed with a 6 × 3 m quiet-zone with an operating frequency in the range from 1–40 GHz to realize antenna characteristics measurement. The profile of the CTR is an offset rotating paraboloid, as shown in figure 5, and the geometric parameters of the reflector are the following.

$F = 10000$ mm, focal length,

$W = 12000$ mm, width in XY projection plane,

$H = 7000$ mm, height in XY projection plane,

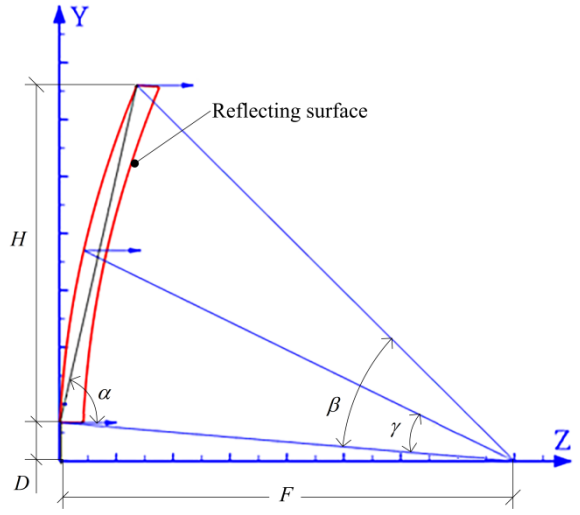

Figure 5. Electrical design parameters of the reflector.

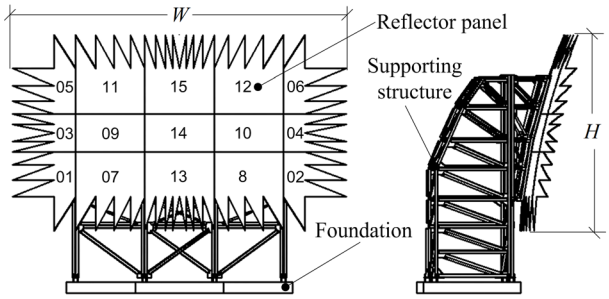

Figure 6. Structure of the reflector and supporting structure.

$A = 1000$ mm, vertical distance from lower edge to vertex,
$\alpha = 77.320°$, Tilt angle of reflector,
$\beta = 37.878°$, Irradiation angle of feed horn,
$\gamma = 25.361°$, elevation angle of feed horn.

Considering the capability of the forming equipment and geometric size of the reflector, the entire reflector was divided into 15 sub-panels to be separately manufactured. Figure 6 shows the separation scheme of the reflector and the structure of the supporting stand. The reflector is designed in the form of a sandwich structure, referring to two layers of honeycomb sandwiched between three layers of aluminum skins, also featuring high specific stiffness and good electrical properties [20]. Four Φ1.2 mm small holes called mark points were machined to mount 0.5-inch TBR on the front of each sub-panel, and similarly, four Φ2.0 mm holes were drilled to locate the adjustment mechanism at the projection position on the back of each sub-panel.

3.2. Problem description

To guarantee the permanent stability of electromagnetic performance of the CTR, reinforced concrete is generally adopted to form the foundation of the CTR reflectors, and the depth of the foundation is determined by geological conditions, also treated specifically to isolate vibration from the surroundings. However, the foundation of the CTR reflector faces certain risks at the beginning of design, which was built

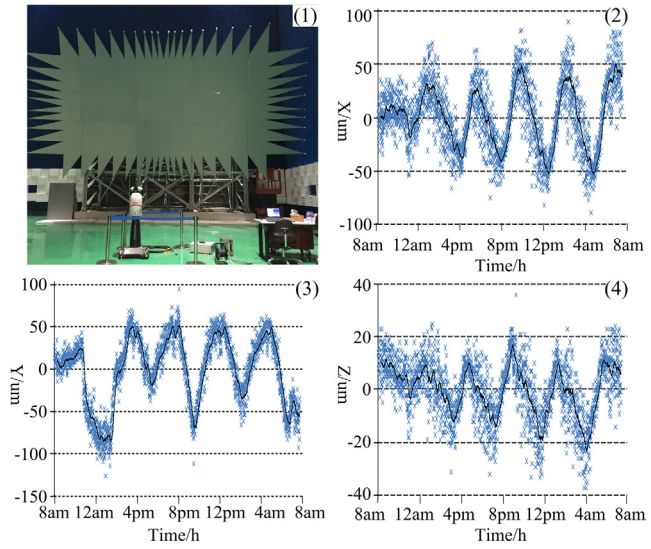

Figure 7. Actual measurement uncertainty of laser tracker at on-site alignment environment with temperature(21 °C ± 3 °C) and humidity (50% ± 20%) and no-isolation foundation.

on concrete floor with the depth of 400 mm but without vibration isolation from the surroundings. We found that the MCS of the laser tracker has a positional fluctuation over time with respect to the DCS of the reflector during the alignment process. To explore the cause of the fluctuation between the MCS and DCS, we operated the laser tracker (Leica, AT901-B) to dynamically monitor and measure one point placed on the supporting structure lasting 24 h at the alignment site. The point was measured every 30 s, and the measurement distance is approximately 10 m. Finally, more than 2800 sets of data collected were statistically analyzed to evaluate the fluctuation of the MCS. The measurement process and X, Y, Z coordinate fluctuations are shown in figure 7. Comparing figures 3 and 7, the on-site measurement uncertainty of the laser tracker is higher than the laboratory uncertainty. This shows that the on-site environment of assembly and alignment of reflector panels is a non-ideal measurement environment, perhaps because of the non-isolated foundation. The fluctuation of the MCS is fatal to the on-site alignment of the reflector panels. Therefore, iterative regression must be performed to unify the MCS according to the alignment flow shown in figure 2.

3.3. Alignment process

Therefore, the adjustment of the alignment for this project still utilizes a closed-loop system. The process is as follows.

Step 1—MCS establishment: With the employment of electronic theodolite, the MCS based on a laser tracker is established, the $X_D OZ_D$ plane of which is supposed to be parallel to the horizontal plane. The laser tracker is placed along the focal axis of the reflector and located between the reflector and the feed.

Step 2—Installation and approximate alignment: First, each reflector panel is installed on the supporting structure by four adjustment mechanisms, with the ability of adjustment in six DOFs for each panel. Then, all these panels are approximately

aligned and located to their design positions, and the initial adjustment value $\Delta \boldsymbol{X}_1$ is calculated by

$$\Delta \mathbf{X}_1 = \mathbf{X}^{\mathrm{D}} - \mathbf{X}^{\mathrm{M}} \tag{24}$$

where, $\mathbf{X}^{\mathrm{D}}$ and $\mathbf{X}^{\mathrm{M}}$ is the design coordinate value and real-time measuring value of mark points, respectively. After the approximate alignment, the deviation $|\Delta \mathbf{X}_1|$ is controlled within 0.5 mm, and the gap between adjacent panels is within 0.4 ± 0.2 mm. The approximate alignment does not needs to take the influence of foundation oscillation into account because the requirement of position accuracy in this stage is not strict.

Step 3—On-site accurate alignment: Point-cloud data of each panel are collected using the dynamic scanning measurement of the laser tracker. The collected data is then best fitted with its design surface. The best-fitting process is formulated as follows.

$$\min \sum_{i}^{n} \left\| \left(\mathbf{R}' \mathbf{X}_j' + \mathbf{T}' \right) - f\left(\mathbf{X} \right) \right\|^2 \tag{25}$$

in which

$$\mathbf{X}_j' = \mathbf{R}_0 \mathbf{X}_j + \mathbf{T}_0 \tag{26}$$

where $\mathbf{X}_j$ is the measurement data of the reflection surface, and $f\left(\mathbf{X}\right)$ the design equation of the reflector. The rotation matrix $\mathbf{R}_0$ and transfer matrix $\mathbf{T}_0$ are the drift of the MCS caused by the non-metrology environment. The rotation matrix $\mathbf{R}'$ and transfer matrix $\mathbf{T}'$ can be identified by solving (25), and the adjustment value $\Delta \mathbf{X}_2$ of each adjustment mechanism can be calculated as follows:

$$\Delta \mathbf{X}_2 = \left(\mathbf{R}' \mathbf{X}_{p,i} + \mathbf{T}' \right) - \mathbf{X}_{p,i} \tag{27}$$

where, $\mathbf{X}_{p,i}$ is the real-time measurement value of the mark points. On-site accurate alignment will be carried out by the alignment of each adjustment mechanism according to the calculated value. The deviation $|\Delta \mathbf{X}_2|$ should be controlled within 0.01 mm.

Step 4—Location of feed: Final measurement data of actual surface of the reflector are used to best fit paraboloid, and the fitting focus of the reflector is obtained. According to the fitting focus, the center of the feed horn is adjusted and aligned by the laser tracker. The adjustment value $\Delta \mathbf{X}_3$ is calculated as follows:

$$\Delta \mathbf{X}_3 = \mathbf{X}_{\mathrm{F}}^{\mathrm{F}} - \mathbf{X}_{\mathrm{F}}^{\mathrm{M}} \tag{28}$$

where $\mathbf{X}_{\mathrm{F}}^{\mathrm{F}}$ is the coordinate value of the fitted focus and $\mathbf{X}_{\mathrm{F}}^{\mathrm{M}}$ the real measurement value of the focus of the feed.

3.4. Alignment results

At the beginning of the alignment of the reflector panels, 12 common points were set on the ground to unify the coordinate system according to the method mentioned in [15, 18]. First, we aligned the 13#, 14#, and 15# panels using the iterative alignment system, and the RMS value of deviation arrived at 38 μm, as shown in figure 8(a). However, the RMS value increases to 59 μm after aligning coordinate system using the 12 common points on the following day, and the deviation was shown in figure 8(b). In this case, the alignment of the remaining reflector panels cannot be continued. To solve this problem, we conducted a lot of tracking measurement experiments. Through tracking measurement experiments, we found that selecting the modified marked points on the panels to alignment the coordinate could get better results with RMS value 41 μm in figure 8(c). The error of coordinate alignment using the exiting methods is 21 μm, and the error using the proposed method only 3 μm. Results show that the method of coordinate alignment proposed in this paper can effectively solve the alignment problem of reflector panels in the oscillation environment.

Owing to the oscillation of the assembly and alignment site, the MCS must be aligned several times during the alignment process. However, each MCS regression will introduce a new error because of the measurement uncertainty of the laser tracker. The regression error of MCS was evaluated using the Monte Carlo method based on the measurement error model of the laser tracker. Approximately 1000 sample data were randomly selected from the error model to calculate the regression error of the MCS per unit of time. The reference points of the reflector panels used for MCS registration are shown in table 1. The ideal coordinate values of reference points shown in the table are obtained when the actual and theoretical profiles of the panel are best matched. The regression error obtained by the Monte Carlo method is shown in figure 9. The RMS value of the alignment error introduced by single MCS alignment is approximately between 3 and 8 μm. The simulation results of MCS alignment error were tested and verified using laser tracker at alignment site. As can be seen from figure 9, the maximum deviation between the simulated and experimental values of regression error is 8 μm. This shows that the measurement uncertainty model of the laser tracker established in this paper is accurate.

In the actual alignment process, the number of MCS alignments should be controlled as much as possible due to the existence of measurement errors. Through comprehensive analysis of regression errors and coordinate fluctuations at the alignment site, the alignment strategy of the MCS was formulated. The approximate alignment does not need MCS regression because the requirement of position accuracy in this stage is not strict. After approximate alignment, the RMS value of the deviation between the actual and theoretical profiles is 147 μm, as shown in figure 10.

The first MCS alignment was carried out by four reference points of the 14# panel. After the first regression, the 9# and 10# panels were aligned to their theoretical models. The second regression used 12 reference points of the 09#, 10#, and 14# panels, and then the 13# and 15# panels were aligned to their theoretical models. Next the third alignment by 20 points from the 09#, 10#, 13#, 14#, and 15# panels. In this step, four panels numbered 07#, 08#, 11#, and 12# were aligned to their theoretical models. The actual profile data of the middle nine panels were measured by a

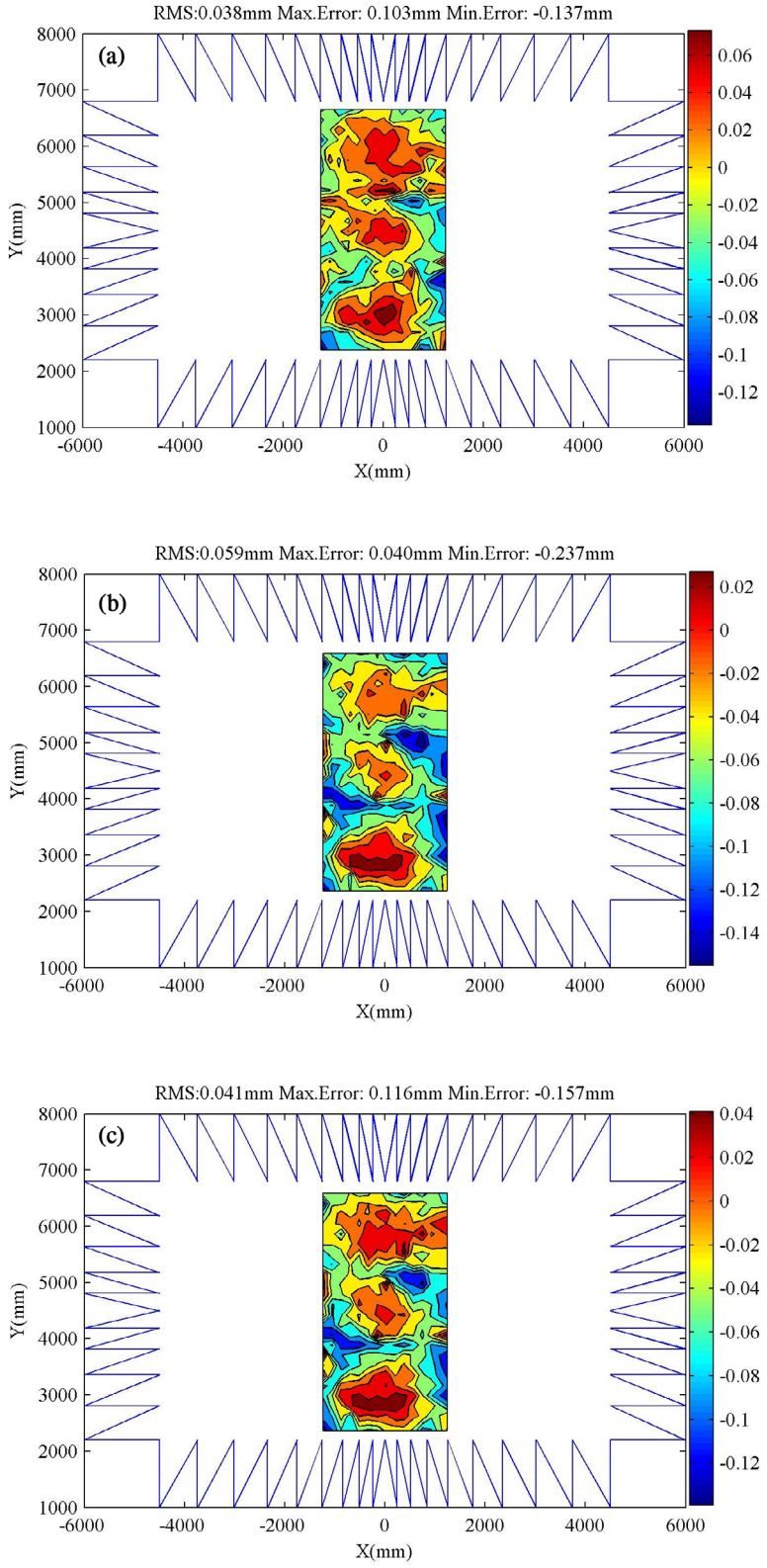

Figure 8. Surface deviation of the 13#, 14#, and 15# panels. (a) Alignment deviation at the beginning. (b) Alignment deviation after unifying by 12 common points on the ground. (c) Alignment deviation after unifying by modified marked points on the panels.

Table 1. Ideal coordinate values of reference points placed on reflector panels.

RP	Ideal coordinate value (mm)			RP	Ideal coordinate value (mm)		
	x	*y*	*z*		*x*	*y*	*z*
09#-P1	−3187.1570	4119.8939	687.6056	10#-P1	1807.1217	4119.6944	515.1805
09#-P2	−3187.1059	4875.3966	857.6407	10#-P2	1807.0730	4875.2157	685.1479
09#-P3	−1806.8848	4875.1591	685.2385	10#-P3	3187.0361	4875.4240	857.5983
09#-P4	−1807.1516	4119.7638	515.2229	10#-P4	3187.1840	4120.0219	687.6369
13#-P1	−696.1940	2558.4987	184.8774	14#-P1	−696.0747	4119.7283	445.7919
13#-P2	−696.4016	3457.9554	320.1990	14#-P2	−696.4290	4875.1685	615.6339
13#-P3	696.6116	3457.8882	320.2275	14#-P3	696.5736	4875.0859	615.6552
13#-P4	696.6414	2558.4822	184.9121	14#-P4	696.6088	4119.8634	445.6868
15#-P1	−696.8795	5537.1924	788.1397	15#-P2	−696.4445	6516.5551	1083.2379
15#-P3	696.6169	6516.5669	1083.4492	15#-P4	696.2723	5536.7302	788.0558

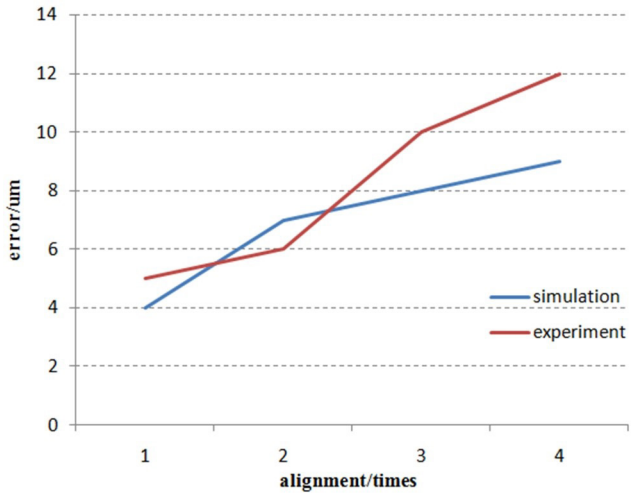

Figure 9. Simulation and experimental error of the MCS alignment.

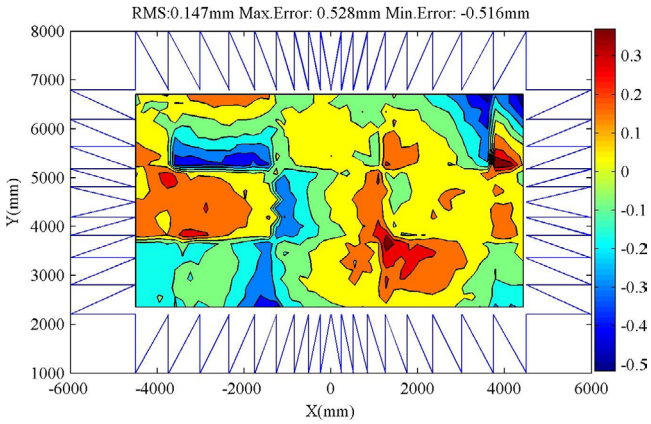

Figure 10. Surface deviation of the whole reflector after approximate alignment.

laser tracker, and compared with their theoretical model. Further adjustment of the panel with large deviation from the theoretical profile was carried out carefully. Finally, six panels on both sides were aligned. Through assembly and alignment lasting for 3 weeks, the 15 sub-panels of the CTR reflector were aligned to their nominal models. The final RMS value

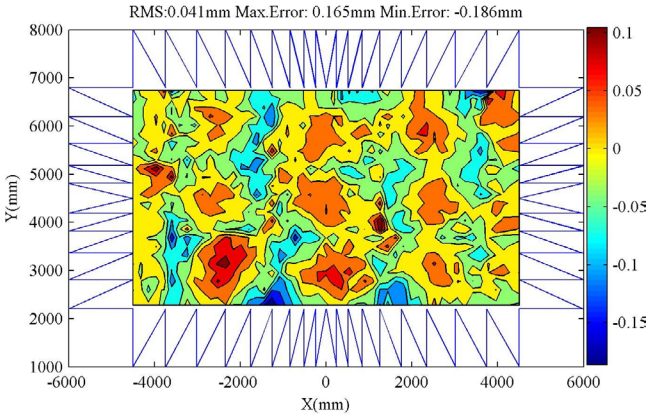

Figure 11. Final surface deviation of the whole reflector.

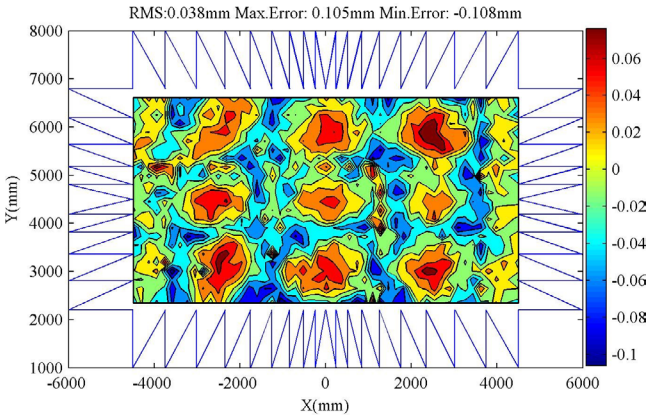

Figure 12. Manufacturing deviation of the whole reflector.

of the deviation between the actual profile and theoretical profile of the entire reflector reached 0.041 mm, as shown in figure 11. The manufacturing deviation of the whole reflector is 0.038 mm, as shown in figure 12. The loss of accuracy caused by on-site alignment is only 7.9% of the theoretical value. The gap between adjacent panels was measured by a plug gauge, and controlled within 0.08–0.75 mm, as shown in figure 13. The deviation in the direction of the crosshairs is shown in figure 14, and the maximum deviation is 0.082 mm

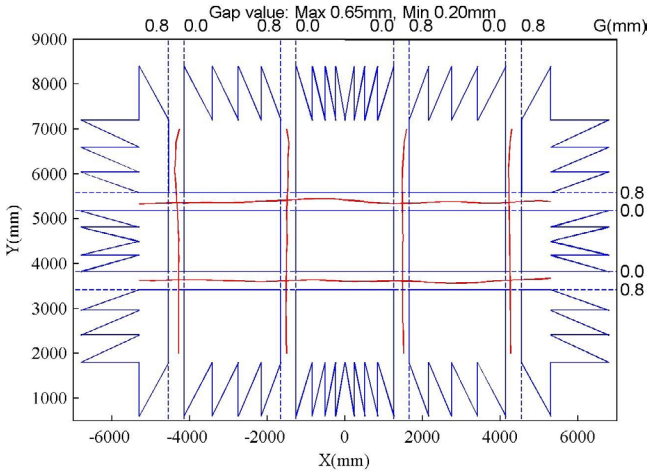

Figure 13. The gap between adjacent panels.

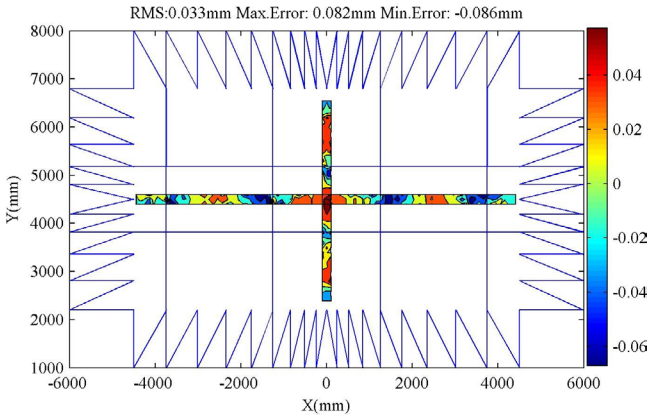

Figure 14. The deviation in the direction of the crosshair.

Figure 15. Live pictures of reflector assembly and alignment.

and the minimum deviation −0.086 mm. Several live photographs of assembly and alignment are shown in figure 15. From the alignment results of the reflector panels, the iterative alignment system and MCS regression method proposed in this paper are very effective.

Finally, the phase center of the feed horn is adjusted by utilizing the laser tracker, and its design position, fitting position and actual position are shown in table 2.

Table 2. Position of focal point of the reflector.

Phase center	*X* (mm)	*Y* (mm)	*Z* (mm)
Design value	0	0	10 000
Fitting value	−1.134	−0.349	10 000.190
Actual value	−1.073	−0.289	10 000.166
Position error	0.061	0.060	−0.024

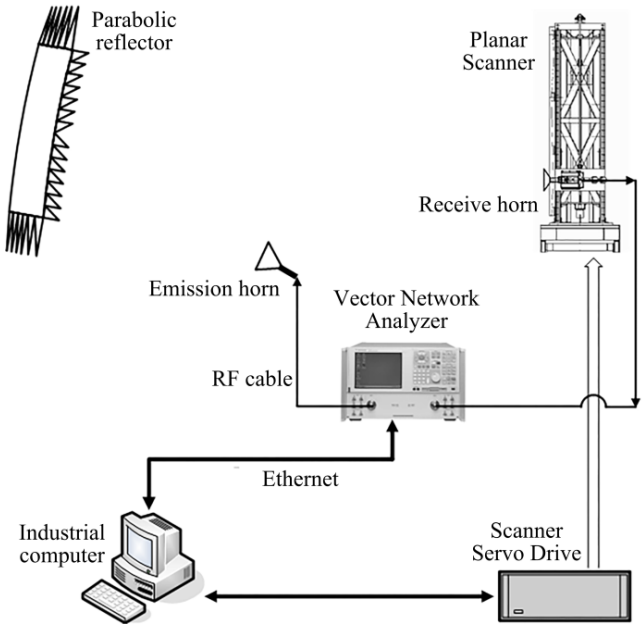

Figure 16. Microwave test system based on probe scanning method.

3.5. Electromagnetic performance test of the CTR

There are many factors affecting the electromagnetic performance of the CTR, such as the surface accuracy of the reflector, geometric design of the darkroom, shielding properties, and type and layout of absorbing material. To evaluate the electromagnetic performance within the quiet zone of the CTR, a microwave amplitude and phase test system based on probe scanning was established using a high-accuracy planer scanner, as shown in figure 16. The characteristics of magnitude, taper, and cross-polarization within the quiet zone were tested on eight frequency bands, such as L, S1, S2, C, Xc, Ku, K, and Ka, with three frequency points for each band. Figure 17 shows the curve of amplitude and phase performance at 25 GHz and table 3 the cross-polarization features. The test results indicate that the overall electrical design of the CTR is satisfactory, and the precision of the reflector surface can meet the requirement of the 40 GHz operating frequency.

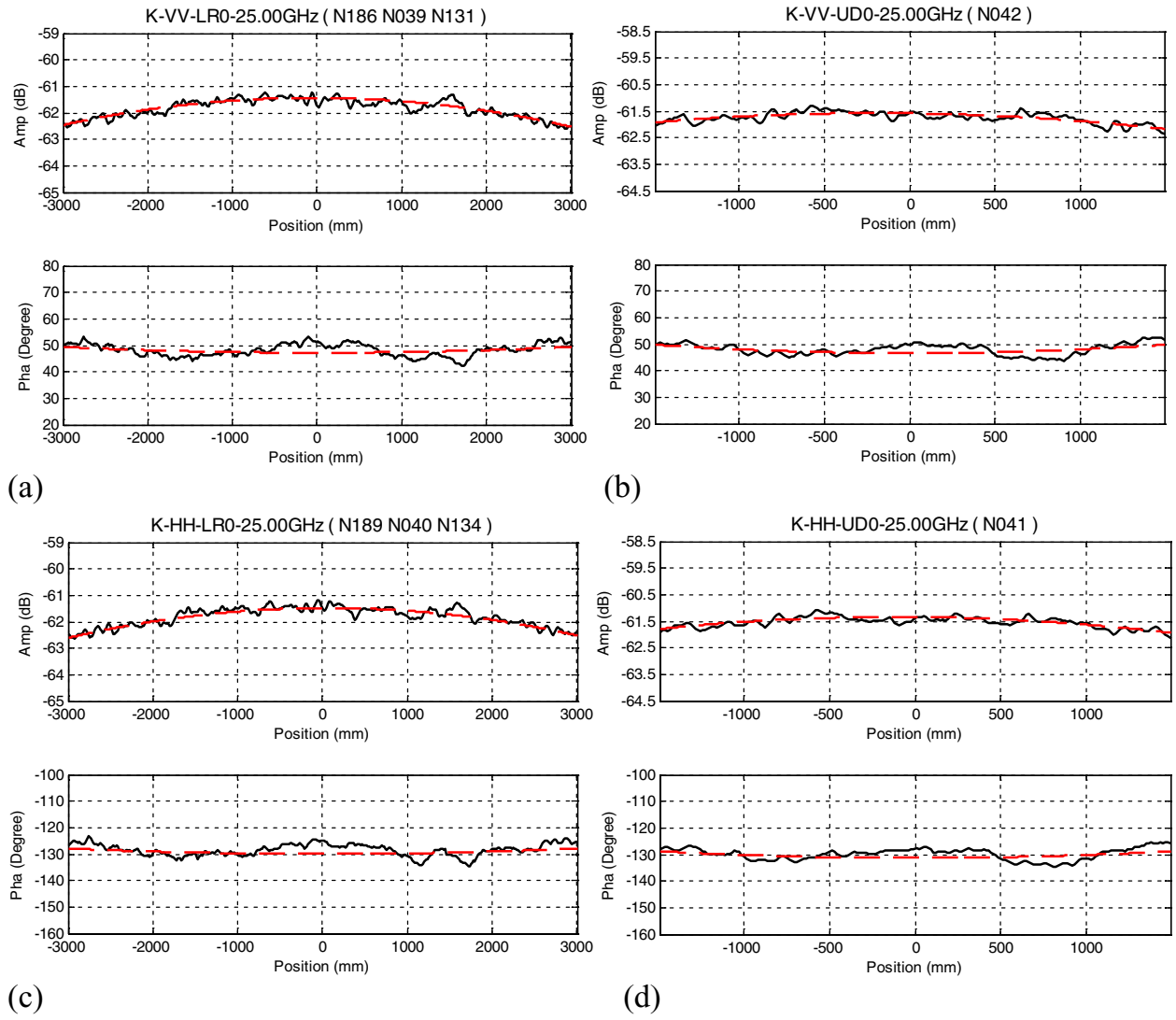

Figure 17. Amplitude and phase characteristics at 25 GHz. (a) VV polarization, horizontal scanning line, (b) VV polarization, vertical scanning line, (c) HH polarization, horizontal scanning line, (d) HH polarization, vertical scanning line.

Table 3. Test results of cross polarization.

Band	Freq (GHz)	HV (dB)		VH (dB)	
		L	*R*	*L*	*R*
L	1.4	−46.0	−31.5	−26.9	−29.1
S1	2.5	−33.9	−35.2	−46.0	−32.0
S2	3.3	−40.9	−39.6	−40.8	−49.0
C	4.9	−36.4	−47.5	−37.4	−39.1
Xc	7	−37.3	−41.5	−41.4	−37.1
X	10	−41.2	−36.7	−37.4	−43.1
Ku	15	−42.8	−35.0	−34.9	−45.9
K	22	−40.5	−31.6	−33.0	−40.8
Ka	33	−34.0	−38.4	−38.9	−31.3

4. Conclusion

An iterative alignment system was established based on a commercial laser tracker and a 6-DOF adjustment mechanism, which successfully assembled and aligned 15 sub-panels of a CTR reflector with 12 m width and 7 m height in a non-metrology environment. The final surface accuracy of the CTR reflector reached 0.041 mm and the loss precision of the reflector caused by alignment was only 7.9%. The alignment method was developed to unify the MCS based on iteratively adding and modifying reference points placed on aligned reflector panels. Because of the reference points placed on the aligned panels could be consistent with the changes of the reflector caused by environmental factors, the greater significance is that this method can effectively eliminate the influence of a non-metrology environment on coordinate unification, such as foundation oscillation, temperature variation, and humidity change. The actual uncertainty model of the laser tracker was created according to a large amount of field measurement data to evaluate alignment error using the Monte Carlo method. Comparing the test and simulation results, the actual uncertainty model of the laser tracker is accurate.

Finally, a microwave amplitude and phase test system based on probe scanning was established using a high-accuracy planer scanner to evaluate electromagnetic performance

within the quiet zone of the CTR. The characteristics of magnitude, taper, and cross-polarization within the quiet zone were tested on eight frequency bands, such as L, S1, S2, C, Xc, Ku, K, and Ka, with three frequency points for each band. Results show that the overall electrical design of the CTR is satisfactory, and the precision of the reflector surface can meet the requirements of the 40 GHz operating frequency.

Acknowledgments

This research work is sponsored by the National Natural Science Foundation of China (Grant Nos. 51575028). I would like to extend my sincere gratitude to Mr Chang Hesheng, Dr Zhou Guofeng and Mr Yu Hongjiang for their valuable guidance in the implementation phase of the project.

The authors have confirmed that any identifiable participants in this study have given their consent for publication.

ORCID iDs

Mingming Wang https://orcid.org/0000-0002-6971-7232

References

[1] Panin S B, Tuchkin Y A, Poyedinchuk A E and Unal I 2018 Axially symmetric compact range reflectors: application of the analytic regularization method *Acoust. Phys.* **64** 150–7

[2] Parini C, van Rensburg D J, Gregson S and McCormick J 2014 Compact range measurements *Theory and Practice of Modern Antenna Range Measurements* (London: Institute of Engineering and Technology) pp 93–169

[3] Tellakula A, Griffin W R and McBride S T 2017 Quiet zone qualification of a very large, wideband rolled-edge reflector *AMTA 2016 Proc.* (IEEE) 1–6

[4] Zhou G, Li X, Li D, Luan J and Zhao J 2014 Surface accuracy of a large-scale compact antenna test range considering mechanism, metrology and alignment *Meas. Sci. Technol.* **25** 075011

[5] Wang M, Li D, Zhou X and He G 2017 Design, fabrication and on-site alignment of low-cost reflector used in large-scale compact antenna test range *2017 11th European Conf. on Antennas and Propagation (EUCAP)* (IEEE) 2590–4

[6] Crane J A 2000 Alignment measurements of the microwave anisotropy probe (MAP) instrument in a thermal/vacuum chamber using photogrammetry *SPIE Proc.* **4131** 255–65

[7] Guofeng Z, Xiaoxing L, Dongsheng L, Zhigang L and Jingdong L 2015 Large-scale compact range on-site alignment based on laser tracker measurement network *Meas. J. Int. Meas. Confed.* **68** 143–54

[8] Legg T H, Avery L W, Matthews H E and Vallée J P 2004 Gravitational deformation of a reflector antenna measured with single-receiver holography *IEEE Trans. Antennas Propag.* **52** 20–5

[9] Baars J W, Greve A, Hein H, Penalver J, Morris D and Thum C 1994 Design parameters and measured performance of the IRAM 30 m millimeter radio telescope *Proc. IEEE* **82** 687–96

[10] Kesteven M J, Parsons B F and Yabsley D E 1988 Antenna reflector metrology: the Australia telescope experience *IEEE Trans. Antennas Propag.* **36** 1481–4

[11] Grahl B H, Godwin M P and Schoessow E P 1986 Improvement of the effelsberg 100 meter telescope based on holographic reflector surface measurement *Astron. Astrophys.* **167** 390–4

[12] Grattan C L and Bennett J C 2007 Microwave holographic technique for reflector antenna profile measurement *Electron. Lett.* **22** 977

[13] Hunter T R *et al* 2011 Holographic measurement and improvement of the green bank telescope surface *Publ. Astron. Soc. Pacific* **123** 1087–99

[14] Conte J, Majarena A C, Aguado S, Acero R and Santolaria J 2016 Calibration strategies of laser trackers based on network measurements *Int. J. Adv. Manuf. Technol.* **83** 1161–70

[15] Zhao G, Zhang P and Xiao W 2018 Coordinate alignment of combined measurement systems using a modified common points method *J. Instrum.* **13** P03021

[16] Muralikrishnan B, Phillips S and Sawyer D 2016 Laser trackers for large-scale dimensional metrology: a review *Precis. Eng.* **44** 13–28

[17] Zhao G, Zhang C, Jing X, Sun Z, Zhang Y and Luo M 2016 Station-transfer measurement accuracy improvement of laser tracker based on photogrammetry *Meas. J. Int. Meas. Confed.* **94** 717–25

[18] Gale D M 2012 Experience of primary surface alignment for the LMT using a laser tracker in a non-metrology environment *Ground-based and Airborne Telescopes IV* **8444** 844453

[19] Leon-Huerta A *et al* 2014 Experiences with global laser tracker alignment of the 32.5 m LMT primary surface *Advances in Optical and Mechanical Technologies for Telescopes and Instrumentation* **9151** 91513Q

[20] Changling H, Xianbin Z and Xiaoqiang L 2009 Solution to boundary-value problems in fabrication of high-precision reflector panels *Chin. J. Aeronaut.* **22** 97–104